International Journal of Earth, Energy and Environmental Sciences
ISSN: 2517-942X
Vol:10, No:3, 2016

# An Analysis of the Performances of Various Buoys as the Floats of Wave Energy Converters

İlkay Özer Erselcan, Abdi Kükner, Gökhan Ceylan

***Abstract*****—**The power generated by eight point absorber type wave energy converters each having a different buoy are calculated in order to investigate the performances of buoys in this study. The calculations are carried out by modeling three different sea states observed in two different locations in the Black Sea. The floats analyzed in this study have two basic geometries and four different draft/radius (d/r) ratios. The buoys possess the shapes of a semi-ellipsoid and a semi-elliptic paraboloid. Additionally, the draft/radius ratios range from 0.25 to 1 by an increment of 0.25. The radiation forces acting on the buoys due to the oscillatory motions of these bodies are evaluated by employing a 3D panel method along with a distribution of 3D pulsating sources in frequency domain. On the other hand, the wave forces acting on the buoys which are taken as the sum of Froude-Krylov forces and diffraction forces are calculated by using linear wave theory. Furthermore, the wave energy converters are assumed to be taut-moored to the seabed so that the secondary body which houses a power take-off system oscillates with much smaller amplitudes compared to the buoy. As a result, it is assumed that there is not any significant contribution to the power generation from the motions of the housing body and the only contribution to power generation comes from the buoy. The power take-off systems of the wave energy converters are high pressure oil hydraulic systems which are identical in terms of their characteristic parameters. The results show that the power generated by wave energy converters which have semi-ellipsoid floats is higher than that of those which have semi elliptic paraboloid floats in both locations and in all sea states. It is also determined that the power generated by the wave energy converters follow an unsteady pattern such that they do not decrease or increase with changing draft/radius ratios of the floats. Although the highest power level is obtained with a semi-ellipsoid float which has a draft/radius ratio equal to 1, other floats of which the draft/radius ratio is 0.25 delivered higher power that the floats with a draft/radius ratio equal to 1 in some cases.

***Keywords*****—**Black Sea, Buoys, Hydraulic Power Take-Off System, Wave Energy Converters.

## I. Introduction

WAVE energy is an abundant and promising source of energy among other renewable energy sources. The surface of the oceans and seas are restless most of the time and the waves carry vast amounts of energy. The research activities on generating electricity from the waves have been continuing since the days of the Energy Crisis. The disadvantages of generating most of the energy required for both industrial and daily activities by consuming fossil fuels were seen after the oil supply had decreased and the prices had increased. As a result, new sources and methods of generating the energy needed started to emerge. Ocean waves which are one the renewable energy sources are considered as one of these new sources of energy. Many different types of wave energy converters were designed during the last four decades in order to capture the energy of the waves and then to convert it into electricity. Although they differ in size and shape, their principles of converting the power of waves and mechanisms used in this process are mostly similar.

Point absorber type wave energy converters are those of which the horizontal dimensions of the system are smaller than the wave lengths. A recent study indicates that the number of this type of wave energy converters developed is higher than the number other types of wave energy converters developed so far [1]. Any axi-symmetrical body such as a circular cylinder, a semi-ellipsoid or a semi-elliptic paraboloid can be employed as the float of a wave energy converter. Since there are a number of geometries and possibly a greater number of different dimensions that can be used in the design of the floats, the interactions of these bodies with waves and their capabilities of capturing the power of waves should be studied before deciding on a particular geometry and dimensions. In order to find the best option, various buoys are designed using four different draft/radius ratios and calculations are carried out by modeling three different sea states observed in two separate locations in the Black Sea. The power generated by the power take-off system is calculated for each case and the performances of all buoys are evaluated through these power values.

## II. The Solution of the Problem

The floats of the wave energy converters designed in this study possess the geometries of a semi-ellipsoid and a semi-elliptic paraboloid. The surfaces of an ellipsoid and an elliptic paraboloid can be modeled by using the following equations. *A*, *B*, and *C* are the radii of the body on each axis.

$$\frac{x^2}{A^2}+\frac{y^2}{B^2}+\frac{z^2}{C^2}=1 \quad (1)$$

$$\frac{z}{C}=\frac{x^2}{A^2}+\frac{y^2}{B^2} \quad (2)$$

It is assumed that the systems oscillate only in heave direction and no other motion contributes to power generation.

İlkay Özer Erselcan is Department of Naval Architecture and Marine Engineering, Istanbul Technical University, Maslak, 34469, Istanbul, Turkey (Phone: 0090 553 488 2189; fax: 0090 212 285 6454; e-mail: ioerselcan@itu.edu.tr).

Abdi Kukner is with Department of Naval Architecture and Marine Engineering, Istanbul Technical University, Maslak, 34469, Istanbul, Turkey (e-mail: kukner@itu.edu.tr).

Gokhan Ceylan is with Department of Naval Architecture and Marine Engineering, Turkish Naval Academy, Tuzla, 34940, Istanbul, Turkey (e-mail: gceylan@dho.edu.tr).

While all of the floats have masses which are equal to the mass of a semi-sphere with a radius of 5 meters, their dimensions are different from each other such that the ratios of draft/radius (d/r) are 0.25, 0.5 0.75 and 1. The power take-off system is built from a double acting piston cylinder which is activated by the oscillating float and pumps the hydraulic oil. Additionally, a check valve group serves as a rectifier so that the flow becomes uni-directional. Finally, a hydraulic motor coupled to a generator converts the hydraulic power into mechanical and electrical power. The motions of the buoys are evaluated using both 3D pulsating source distribution method and linear wave theory.

*A. The Hydrodynamic Problem*

The heave motion of the float is solved by employing a 3D pulsating source distribution method. The potential function of a stationary 3D source with pulsating strength in deep water is given as the following in [2].

$$\varnothing = \left[\frac{1}{r}+\frac{1}{r'}+2\nu PV\int_0^\infty \frac{e^{k(z+c)}J_0(kR)}{k-\nu}dk+2\pi i\nu e^{\nu(z+c)}J_0(\nu R)\right]\sigma \quad (3)$$

$$r=\left[(x-a)^2+(y-b)^2+(z-c)^2\right]^{1/2} \quad (4)$$

$$r'=\left[(x-a)^2+(y-b)^2+(z+c)^2\right]^{1/2} \quad (5)$$

$$R=\left[(x-a)^2+(y-b)^2\right]^{1/2} \quad (6)$$

Here, a Cartesian coordinate system is adapted such that *xoy* plane coincides with the undisturbed free surface and positive direction of *z*-axis points upwards. The coordinates (*x*,*y*,*z*) represent a point in the fluid domain and (*a*,*b*,*c*) represent the position of the source in (3)-(6). The wave number is given as $\nu=\omega^2/g$ in deep water where $\omega$ is the wave frequency, $g$ is the acceleration of gravity and $k$ is the integration variable. Moreover, PV stands for Cauchy's Principle Value Integral and $J_0$ is Bessel function of the first kind order zero. Equation (3) satisfies Laplace equation, linearized kinematic and dynamic free surface boundary conditions, bottom boundary condition at infinite depth and radiation condition. The added mass and hydrodynamic damping of a body oscillating with small amplitude at the frequency of incoming regular waves are calculated by satisfying body boundary condition on the surface of the body and by calculating the forces acting on the body due to the oscillations. The solution of the problem is as follows.

First, the surface of the body is divided into triangular panels and constant strength sources are distributed on these panels. Then, (3) and its spatial derivatives are integrated on the triangular panels by a numerical integration method and potential values along with velocity components induced at the centroids of all other panels are obtained.

Dividing the surface of the body into plane surface elements converts the surface integrals evaluated on the entire surface of the body into a sum of integrals evaluated on the surfaces of panels as shown in the following equations:

$$\Phi = \int_{S_{body}} \varnothing dS \cong \sum_{i=1}^{N}\int_{S_{panel}} \varnothing dS \quad (7)$$

$$\vec{\mathrm{V}} = \int_{S_{body}} \vec{\nabla}\varnothing dS \cong \sum_{i=1}^{N}\int_{S_{panel}} \vec{\nabla}\varnothing dS \quad (8)$$

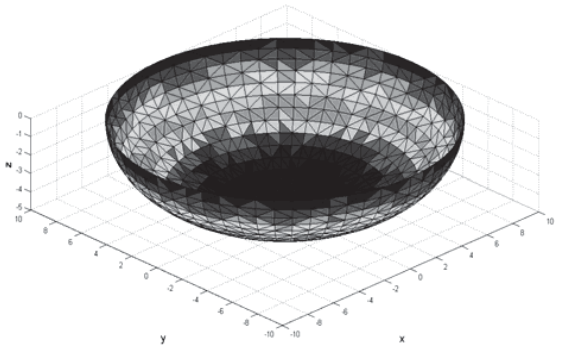

Fig. 1 Triangular surface mesh of a semi-ellipsoid

Since the source strengths are unknown in the beginning, the integrals given in (7) and (8) cannot be fully evaluated. The strengths of the sources are found by solving a system of linear equations. The normal velocities induced at the centroids of panels are calculated by finding the contributions of all panels. So, (7) and (8) are first solved by assuming the source strengths on all panels are unit. Once the contributions of all panels are calculated, a matrix called influence matrix can be formed. Each row of the influence matrix contains the contributions of all panels on the normal velocity induced at the centroid of one panel.

$$I_{jk}=\begin{bmatrix} I_{11} & \cdots & I_{1N} \\ \vdots & \ddots & \vdots \\ I_{N1} & \cdots & I_{NN} \end{bmatrix} \quad (9)$$

Finally, the unknown source strengths are evaluated by satisfying body boundary condition at the centroids of all panels. The normal velocities induced due to the oscillations of the body are calculated by the following equations given in [3] and a column vector $V_n$ which contains the resulting normal velocities due to body motions is formed.

$$V_n=\frac{\partial\varnothing_m}{\partial n}=i\omega n_m \ , \qquad m=1,2,3 \quad (10)$$

$$V_n=\frac{\partial\varnothing_m}{\partial n}=i\omega\left(r\times n\right)_{m-3} \ , \qquad m=4,5,6 \quad (11)$$

The subscript, *m*, represents the motions in six degrees of freedom which are surge, sway, heave, roll, pitch and yaw from one to six, respectively. Additionally, $\varnothing_m$ is the potential of oscillatory motion, $r$ is the position vector with

respect to the origin of the coordinate system, *n* is the unit normal vector pointing out of the body and *i* is the complex unit number. The unknown source strengths are calculated by solving the following equation. The result is a vector which contains the source strengths of all panels.

$$\sigma_k = I_{jk} \setminus V_n \tag{12}$$

Once the unknown source strengths are obtained, the radiation forces acting on the body due to body motions can be found. The resulting forces are complex and functions of wave frequency. The added mass and hydrodynamic damping coefficients can be evaluated by separating real and imaginary parts as described in [3] as:

$$F_{ij} = -\rho \int_{S_B} \frac{\partial \varnothing_i}{\partial n} \varnothing_j dS \quad , i, j = 1, 2, \ldots 6 \tag{13}$$

$$F_{ij} = \omega^2 A_{ij} - i\omega B_{ij} \tag{14}$$

Here, $\varnothing_i$ and $\varnothing_j$ are the oscillation potential of bodies, $A_{ij}$ is the added mass, and $B_{ij}$ is the damping coefficient matrices. Furthermore, the wave forces are calculated by integrating the pressure on the surface of the body due to incoming and diffracted waves. The wave forces acting on the body due to undisturbed incoming waves are known as Froude-Krylov forces and are evaluated as:

$$F_3^{FK}(\omega) = -\rho \int_S \frac{\partial \varnothing_I}{\partial t} n_3 dS \tag{15}$$

where the incident wave potential is given as:

$$\varnothing_I = \frac{iAg}{\omega} e^{kz} e^{-ik(x\cos\beta + y\sin\beta)} \ , \ k = \frac{\omega^2}{g} \tag{16}$$

On the other hand, the presence of the body disturbs the waves and causes them to spread around. The diffraction potential is evaluated by satisfying the following equation on the surface of the body:

$$\frac{\partial \varnothing_D}{\partial n} = -\frac{\partial \varnothing_I}{\partial n} \tag{17}$$

The diffraction potential and resulting forces are evaluated by using the influence matrix given in (9). This time, the normal velocities induced by the incident waves take place in the normal velocity vector $V_n$. Once the wave forces, added mass, hydrodynamic damping coefficients and hydrostatic restoring forces are obtained, the amplitudes of the motions can be found by solving an equation of motion either in frequency domain or in time domain. The motion of a float is evaluated in time domain in this study.

The time domain calculations are carried out by evaluating Cummins equation given in [4], [5] which is widely used in the calculation of ship motions. This equation can be written for heave motion as:

$$\left(M + A_{33}^{\infty}\right)\ddot{x}_3(t) + \rho g S x_3(t) + \int_{-\infty}^{t} h_{33}(t-\tau)\ddot{x}_3(t)\,d\tau = F_3^{FK}(t) + F_3^{D}(t) + F_{PTO}(t) \tag{18}$$

Here, *M* is the mass of the float, $A_{33}^{\infty}$ is heave added mass at infinite frequency, *S* is the water plane area of the float and $h_{33}$ is the memory function for heave acceleration. On the other hand, $F_3^{FK}$ and $F_3^{D}$ are Froude-Krylov and diffraction forces acting on the float in the heave mode of motion in time domain. Since the irregular sea states can be represented by the superposition of regular wave components, these forces can also be calculated approximately by superposition of wave forces which correspond to regular wave components.

$$F_3^{FK}(t) = \sum_{j=1}^{N} F_{3,j}^{FK}\left(\omega_j t + \varepsilon_j\right) \tag{19}$$

$$F_3^{D}(t) = \sum_{j=1}^{N} F_{3,j}^{D}\left(\omega_j t + \varepsilon_j\right) \tag{20}$$

In addition to wave forces, $F_{PTO}$ represents the reaction force acting on the float due to the presence of the power take-off system. Finally, the memory function which is present in the convolution integral in (18) is given as:

$$h_{33}(t) = \frac{2}{\pi}\int_0^{\infty}\left(A_{33}(\omega) - A_{33}^{\infty}\right)\cos(\omega t)\,d\omega = \frac{2}{\pi}\int_0^{\infty}\frac{B_{33}(\omega)}{\omega}\sin(\omega t)\,d\omega \tag{21}$$

Here, $A_{33}$ and $B_{33}$ are heave added mass and hydrodynamic damping of the float, respectively.

The output of the 3D model is first compared to some published results. The surge and heave added mass and hydrodynamic damping coefficients of a semi-sphere oscillating in deep water are compared to the values given in [6]. It can be seen from Fig. 2 that the numerical results obtained by 3D pulsating source distribution method and analytical results are in very good agreement. Additionally, the same solution method is applied to a number of semi-ellipsoids with various length/beam ratios and the coupled heave and pitch motions of these bodies in deep water are calculated in head seas at zero forward speed [7]. This study aimed to investigate the extent of slender body approximation made in linear strip theory by comparing the results of 2D and 3D source distribution methods. It was determined that the results obtained by 3D pulsating source distribution method converged to the results obtained by 2D linear strip theory with increasing length/beam ratio.

*B. Power Take-Off System*

The power take-off system of the wave energy converters considered in this study is a high pressure oil hydraulic system. The hydraulic oil is pumped into the circuit by the piston cylinder activated by the oscillating buoy. A double acting piston is adapted to the power take-off system so that the hydraulic fluid is pumped into the circuit in both up and down strokes of the piston. The pumping of the hydraulic fluid in both strokes creates a bi-directional flow. This two way flow is converted into uni-directional flow by a group of check valves which allow the fluid to flow only in one direction. As a result, the hydraulic motor is supplied with oil almost during the whole period of the motion. A schematic view of a hydraulic power take-off system is shown in Fig. 3.

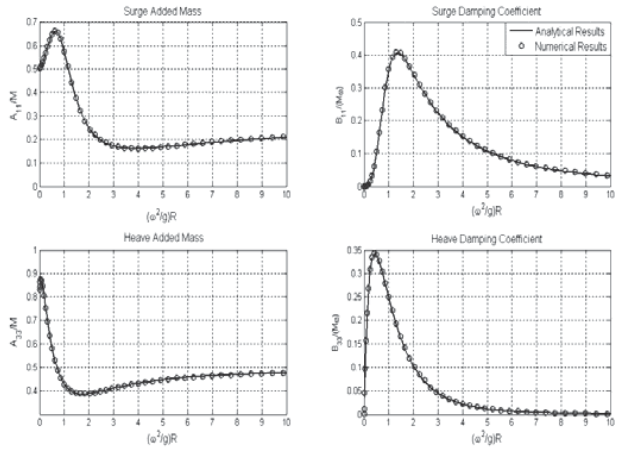


Fig. 2 Surge and heave added mass and damping coefficients of a semi-sphere

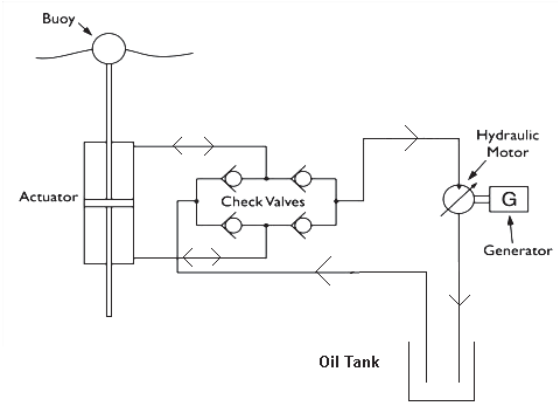


Fig. 3 Schematic of a hydraulic power take-off system [8]

The acceleration and the velocity of the buoy determine the pressure and the flow rate of the hydraulic fluid. The flow rate of the hydraulic fluid can be calculated as:

$$\dot{Q}(t) = \dot{x}_3(t) A_p \tag{22}$$

Here, $\dot{Q}$ represents the instantaneous flow rate, $\dot{x}_3$ is the heave velocity of the buoy and $A_p$ is the effective cross sectional area of the piston.

$$A_p = \frac{\pi}{4}\left(d^2_{piston} - d^2_{rod}\right) \tag{23}$$

The pressure acting on the fluid by the piston depends on the heave force that the buoy exerts on the piston due to acceleration of the heaving motion. Assuming the amplitude of the oscillations of the buoy is small, the absolute pressure acting on the pressure side of the cylinder can be written as:

$$P_{press.side} = \frac{\left(M + A_{33}^{\infty}\right)\ddot{x}_3(t)}{A_p} + p_{atm} \tag{24}$$

On the other hand, if the pressure on the suction side of the cylinder is assumed to be approximately equal to atmospheric pressure since that side is connected to an oil tank which is generally open to atmosphere in practice, the net force acting on the float through the piston becomes approximately equal to

$$F_{PTO}(t) \cong \left(M + A_{33}^{\infty}\right)\ddot{x}_3(t). \tag{25}$$

This reaction force always acts in the opposite direction of the piston's movement. When the piston moves downward, the high pressure will build up in the lower side of the piston head while the low pressure will act from the upper side.

The pressure of the fluid drops while flowing in the power take-off system. The friction of the fluid with the inner surface of the pipes, bends and valves are examples of this pressure loss. The pressure loss in the check valves are calculated as:

$$\Delta p_{cv} = \frac{\dot{Q}^2 \rho}{2 C_d^{\,2} A_v^{\,2}} \tag{26}$$

Here, $C_d$, $A_v$, and $\rho$ represent the valve discharge coefficient, the cross sectional area of the valve and the density of hydraulic fluid, respectively. Equation (26) is known as the orifice equation.

Finally, the hydraulic motor converts the hydraulic power into mechanical power and it can be calculated as:

$$P_{motor} = \eta_{motor} \Delta p_{motor} \dot{Q} \tag{27}$$

where $\eta_{motor}$ and $\Delta p_{motor}$ represent the total efficiency and the pressure differential of the hydraulic motor.

*C. The Black Sea Wave Energy Spectrum*

A research project had been carried out between 1994 and 2001 which aimed to investigate the characteristics of waves

generated by the wind in the seas surrounding Turkey. The wave measurements recorded by buoys deployed in the Eastern Black Sea region were then analyzed and parameters of both Pierson-Moskowitz (PM) spectrum for fully developed seas and JONSWAP spectrum for developing seas were presented for the measured wave data in [9] and [10]. The form of JONSWAP spectrum used in the calculations and the mean values of the parameters of the spectrum for developing seas in two locations in the Eastern Black Sea coast of Turkey are given as follows, respectively.

$$S(f) = \alpha g^2 (2\pi)^{-4} f^{-5} e^{\left\{-1.25\left(\frac{f}{f_p}\right)^{-4}\right\}} \gamma^{e^{\left\{-\frac{(f-f_p)^2}{2\sigma^2 f_p^2}\right\}}} \quad (28)$$

Here, $f_p$ is the peak frequency of the spectrum, $f$ is the frequency of waves in Hz, $g$ is the acceleration of gravity, γ is peak enhancement factor and σ is given as:

$$\sigma = \begin{cases} \sigma_a = 0.07 \ , & f \le f_p \\ \sigma_b = 0.09 \ , & f > f_p \end{cases} \quad (29)$$

TABLE I
MEAN SPECTRAL PARAMETERS OF JONSWAP SPECTRUM FOR THE MEASURED WAVE DATA IN THE EASTERN BLACK SEA

| Location | Sea State | Hs (m.) | A | $\gamma$ | $f_p$(Hz) |
|---|---|---|---|---|---|
| Sinop | 1 | 1.0≤Hs≤2.0 | 0.00507 | 2.57 | 0.162 |
| | 2 | 2.0≤Hs≤3.0 | 0.00622 | 2.34 | 0.127 |
| | 3 | Hs ≥ 3.0 | 0.00884 | 2.74 | 0.120 |
| Hopa | 1 | 1.0≤Hs≤2.0 | 0.00319 | 3.01 | 0.140 |
| | 2 | 2.0≤Hs≤3.0 | 0.00443 | 2.96 | 0.119 |
| | 3 | Hs ≥ 3.0 | 0.00511 | 2.97 | 0.102 |

The irregular waves are modeled by first discretizing the spectrum and then applying the principle of superposition since the wave amplitudes are assumed small compared to wave lengths. A 30-minute period (T) is taken as the duration of the calculations and the time series of irregular waves are obtained by a precision of 0.01 second. Finally, the frequencies of regular wave components are calculated as [11]:

$$\omega_n = \frac{2\pi n}{T}, n = 1, 2, 3, \ldots, \infty \quad (30)$$

## III. RESULTS AND DISCUSSION

The power generated by a wave energy converter is calculated by solving a hydrodynamic problem corresponding to the heave motion of the float which is coupled to the problem associated with the power generation of the power take-off system and the resulting force acting on the float. The motion of the float is solved by assuming that the float is stationary at *t=0*.

The power generated by each wave energy converter in three sea states can be seen in Tables II-V.

The power values given in the tables are the time averages of the instantaneous power levels.

$$\bar{P} = \frac{1}{T}\int_0^T P(t)\,dt \quad (31)$$

TABLE II
POWER (KW) GENERATED IN SINOP BY WAVE ENERGY CONVERTERS WITH SEMI-ELLIPSOID BUOYS

| Sea State | d/r | | | |
|---|---|---|---|---|
| | 1 | 0.75 | 0.5 | 0.25 |
| 1 | 144.8 | 138.9 | 124.3 | 113.4 |
| 2 | 334.3 | 298.9 | 278.3 | 315.4 |
| 3 | 537.5 | 486.9 | 459.8 | 533.9 |

TABLE III
POWER (KW) GENERATED IN HOPA BY WAVE ENERGY CONVERTERS WITH SEMI-ELLIPSOID BUOYS

| Sea State | d/r | | | |
|---|---|---|---|---|
| | 1 | 0.75 | 0.5 | 0.25 |
| 1 | 177.2 | 148.7 | 132.6 | 143.9 |
| 2 | 266.5 | 240.6 | 229.2 | 270.5 |
| 3 | 379.9 | 351.9 | 339.3 | 408.5 |

TABLE IV
POWER (KW) GENERATED IN SINOP BY WAVE ENERGY CONVERTERS WITH SEMI-ELLIPTIC PARABOLOID BUOYS

| Sea State | d/r | | | |
|---|---|---|---|---|
| | 1 | 0.75 | 0.5 | 0.25 |
| 1 | 117.3 | 107.1 | 98.4 | 99.7 |
| 2 | 226.7 | 220.1 | 224.9 | 297.7 |
| 3 | 380.2 | 367.3 | 378.3 | 510.0 |

TABLE V
POWER (KW) GENERATED IN HOPA BY WAVE ENERGY CONVERTERS WITH SEMI-ELLIPTIC PARABOLOID BUOYS

| Sea State | d/r | | | |
|---|---|---|---|---|
| | 1 | 0.75 | 0.5 | 0.25 |
| 1 | 108.3 | 102.2 | 103.1 | 132.6 |
| 2 | 187.8 | 182.7 | 190.4 | 263.4 |
| 3 | 272.6 | 270.9 | 286.4 | 403.6 |

The results show that the power generated by the wave energy converters with semi-ellipsoid buoys is higher than that generated by wave energy converters with semi-elliptic paraboloid buoys in both locations and in all sea states. The power generated by the wave energy converters follow an unsteady pattern such that it does not steadily increase or decrease by changing draft/radius ratios. One may expect that higher power levels could be obtained with floats being more oblate in all cases since higher wave forces act on them as it can be seen in Fig. 4. Although the wave forces acting on the floats increase with decreasing draft/radius ratios, the added mass and radiation damping values increase, too. As a result, the magnitude of the heave motions of the floats decrease with decreasing draft/radius ratios while the semi ellipsoid buoy and semi-elliptic paraboloid buoy with draft/radius ratios equal to 1 experience the greatest oscillations. While these floats have the greatest oscillations in all cases, it can be seen in Tables II-V that the wave energy converters with floats of

which the draft/radius ratio is 0.25 generated higher power than those with a draft/radius ratio equal to 1 in some cases. These results are due to the combined effect of heaving acceleration, velocity and total masses of the systems, the parameters which determine the force exerted to power take-off systems by the floats and the rate of flow resulted in the circuits. Additionally, the wave energy converter with a semi-ellipsoid float of which the draft/radius ratio is 1 delivered the highest power among all other floats in Sinop while the significant wave height is greater than 3 meters, the float which has a draft/radius ratio equal to 0.25 delivered almost the same amount of power in the same sea state. Similar performances can be seen in other sea states and locations as well.

The differences between the added masses, radiation damping values and the wave forces acting on the floats can be seen in Figs. 4-6. The calculations showed that the greatest increase in the wave forces acting on the buoys occur by a factor of approximately 2.5 while both the added mass and the hydrodynamic damping of the buoys increase by a factor of 4. Additionally, it is determined that the magnitude of heave oscillations decrease with decreasing draft/radius ratio in all sea states. All of these parameters determine the amplitudes of waves traveling away from the oscillating bodies in the free surface of a fluid which are also an indicator whether these bodies are good wave energy absorbers or not. Falnes' "a good wave absorber must be a good wave-maker" statement explains this situation [12]. The added mass, damping coefficient and the magnitude of the oscillations are components of radiation force and the magnitude of this force can be considered as a measure of the sizes of the waves traveling away from the oscillating body. The greater the radiation force is, the greater the waves generated due to the oscillations of the body will be. Consequently, all of these parameters determine a body's ability to absorb the energy of waves and to convert it into useful mechanical force for electricity generation.

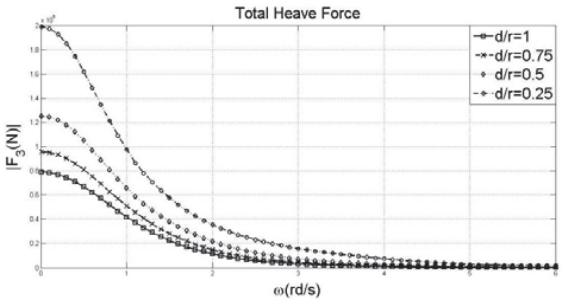


Fig. 4 Total heave forces acting on the buoys

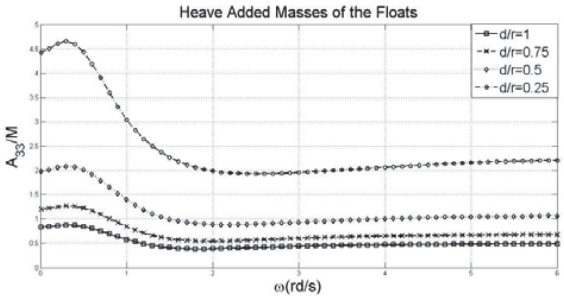


Fig. 5 Added masses of the buoys

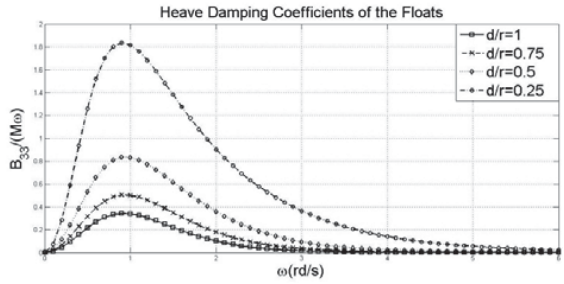


Fig. 6 Hydrodynamic damping of the buoys

## IV. Conclusion

The analysis of the performances of a number of buoys through the power generated by the wave energy converters in three sea states and in two separate locations in the Black Sea showed that the wave energy converter with a semi-elliptic paraboloid buoy with a draft/radius ratio of 0.25 generated the highest power. Although the power values are only presented as an example in order to evaluate the performances of the buoys, these values will be smaller when all losses in the power take-off system are accounted for. Besides modeling the system with more detail, there is one more issue that has to be considered. When wave energy converters take their place in power generation, they are expected to be deployed in arrays. As a result, the interactions of a number of bodies positioned closely to each other will have to be evaluated in order to find an optimum solution for the deployment of these devices and for power generation. The current study is planned to be extended by analyzing the interactions of wave energy converters with each other while they are deployed as an array.

## References

[1] I., Lopez, J. Andreu, S. Ceballos, I.M. Alegria, I. Kortabarria, *Review of wave energy technologies and the necessary power-equipment,* Renewable and Sustainable Energy Reviews, 27, 2013, *pp. 413-434.*

[2] J.V. Wehausen, E.V. Laitone, *Surface Waves Online*, Regents of the University of California, 2002, pp. 475-477.

[3] J.N. Newman, *Marine Hydrodynamics*. Cambridge, MA and London, England, 1989, *MIT Press, pp.287.*

[4] W.E. Cummins, (1962) *The Impulse Response Function and Ship Motions,* Department of Navy David Taylor Model Basin Hydromechanics Laboratory Research and Development Report, Report 1661, 1962.

[5] D. Bruzzone, A. Grasso, *Nonlinear Time Domain Analysis of Vertical Ship Motions,* Archives of Civil and Mechanical Engineering, Vol.VII, No.4, 2007.
[6] A. Hulme, *The wave forces acting on a hemisphere undergoing forced periodic oscillations*. J. Fluid Mech., 1982, Vol.121, pp. 443-463.
[7] İ.O. Erselcan, A. Kükner, *The Investigation of the Motions of an Ellipsoid with Various Length-Beam Ratios in Regular Head Waves,* Proc. of INTNAM 2014, pp. 547-555.
[8] B. Drew, A.R. Plummer, M.N. Sahinkaya, *A review of wave energy conversion technology,* Proc. ImechE Vol.223 Part A: J. Power and Energy, 2009, 887-902.
[9] N., Yılmaz, *Spectral Characteristics of Wind Waves in the Eastern Black Sea,* Middle East Technical University, PhD Thesis, 2007.
[10] N. Yılmaz, E. Özhan, *Characteristics of the Frequency Spectra of Wind-Waves in Eastern Black Sea*, Ocean Dynamics, 2014, pp. 1419-1429.
[11] A.R.J.M. Lloyd, *Seakeeping: Ship Behavior in Rough Weather*, Chichester, West Sussex, England, 1989, pp. 97.
[12] J. Falnes, *Ocean Waves and Oscillating Systems,* Cambridge, United Kingdom, 2004, pp. 196.